Mouse models of human *KCNQ2* and *KCNQ3* mutations for benign familial neonatal convulsions show seizures and neuronal plasticity without synaptic reorganization

Nanda A. Singh[1], James F. Otto[2], E. Jill Dahle[1], Chris Pappas[1], Jonathan D. Leslie[3], Alex Vilaythong[4], Jeffrey L. Noebels[4], H. Steve White[2], Karen S. Wilcox[2] and Mark F. Leppert[1]

[1] *Department of Human Genetics and* [2] *Anticonvulsant Drug Development Program, Department of Pharmacology and Toxicology, University of Utah, Salt Lake City, UT 84112, USA*

[3] *Vertebrate Development Laboratory, Cancer Research UK, London, WC2A 3PX, UK*

[4] *Department of Neurology, Baylor College of Medicine, Houston, TX, 77030, USA*

The childhood epilepsy syndrome of benign familial neonatal convulsions (BFNC) exhibits the remarkable feature of clinical remission within a few weeks of onset and a favourable prognosis, sparing cognitive abilities despite persistent expression of the mutant KCNQ2 or KCNQ3 potassium channels throughout adulthood. To better understand such dynamic neuroprotective plasticity within the developing brain, we introduced missense mutations that underlie human BFNC into the orthologous murine *Kcnq2* (Kv7.2) and *Kcnq3* (Kv7.3) genes. Mutant mice were examined for altered thresholds to induced seizures, spontaneous seizure characteristics, hippocampal histology, and M-current properties of CA1 hippocampal pyramidal neurons. Adult *Kcnq2*$^{A306T/+}$ and *Kcnq3*$^{G311V/+}$ heterozygous knock-in mice exhibited reduced thresholds to electrically induced seizures compared to wild-type littermate mice. Both *Kcnq2*$^{A306T/A306T}$ and *Kcnq3*$^{G311V/G311V}$ homozygous mutant mice exhibited early onset spontaneous generalized tonic-clonic seizures concurrent with a significant reduction in amplitude and increased deactivation kinetics of the neuronal M-current. Mice had recurrent seizures into adulthood that triggered molecular plasticity including ectopic neuropeptide Y (NPY) expression in granule cells, but without hippocampal mossy fibre sprouting or neuronal loss. These novel knockin mice recapitulate proconvulsant features of the human disorder yet show that inherited M-current defects spare granule cells from reactive changes in adult hippocampal networks. The absence of seizure-induced pathology found in these epileptic mouse models parallels the benign neurodevelopmental cognitive profile exhibited by the majority of BFNC patients.

(Received 8 April 2008; accepted after revision 13 May 2008; first published online 15 May 2008)
Corresponding author N. A. Singh: Department of Human Genetics, University of Utah, Salt Lake City, UT 84112, USA. Email: nsingh@genetics.utah.edu

Benign familial neonatal convulsions (BFNC [MIM 121200,121201]) is an autosomal dominantly inherited epileptic disorder in which newborns experience several daily partial or generalized seizures during wakefulness and sleep (Rett & Teubel, 1964; Ryan *et al.* 1991; Ronen *et al.* 1993). In the majority of cases, seizures spontaneously remit by 3–4 months yet 16% of BFNC individuals continue to experience one or more seizures during adulthood (Ronen *et al.* 1993; Singh *et al.* 2003). Mutations in either of two homologous potassium channel genes, *KCNQ2* and *KCNQ3*, have been found in patients with BFNC (Biervert *et al.* 1998; Charlier *et al.* 1998; Singh *et al.* 1998; Lucarini *et al.* 2007). The protein products of these genes colocalize and generate the M-current, a critical regulator of action potential firing and neuronal excitability (Wang *et al.* 1998).

An intriguing phenotypic trait of BFNC is that the frequent spontaneous seizures exhibited by the neonates are not generally associated with any developmental sequelae (Ryan *et al.* 1991; Ronen *et al.* 1993). This is in stark contrast to malignant early childhood onset convulsive seizure disorders that can produce neuronal death and synaptic reorganization with subsequent

This paper has online supplemental material.

 DOI: 10.1113/jphysiol.2008.154971

cognitive impairment (Ben-Ari & Holmes, 2006; Blume, 2006). A biological mechanism that explains the lack of seizure-associated damage could point to a powerful therapeutic strategy for mitigating some of the extensive cell death associated with the prevalent forms of early onset malignant epilepsy. Thus far, however, none of the published BFNC mouse models has recapitulated this paradoxical feature.

Mice developed to date consist of a knockout, transgenic and multigenic deletion, all involving only *Kcnq2* and none of which are based on precise human mutations. The first described BFNC model consisted of a *Kcnq2* heterozygous gene knockout in mutant mice that did not exhibit spontaneous seizures like BFNC patients (Watanabe *et al.* 2000). Although the *Szt1* mouse has a spontaneous *Kcnq2* C-terminal deletion, it did not exhibit seizures and at least two other genes including the epilepsy-associated *Chrna4* gene were deleted (Yang *et al.* 2003). In both of these models, homozygous mutant mice were neonatal lethal. A recently described genetically complex mouse model with a conditional dominant negative *Kcnq2* transgene that suppressed the M-current has been reported to have spontaneous seizures, but displayed impairment of hippocampus-dependent memory and profound behavioural hyperactivity, traits that are inconsistent with the human phenotype (Peters *et al.* 2005).

We have generated two independent knockin mouse lines with the same A306T transmembrane *Kcnq2* mutation and the orthologous G311V pore *Kcnq3* mutation found in two carefully characterized large families with BFNC. These loss-of-function mutations were selected because they represent the mainstream clinical features found in the majority of BFNC patients (Ryan *et al.* 1991; Ronen *et al.* 1993) and have been characterized using multiple *in vitro* systems (Schroeder *et al.* 1998; Chung *et al.* 2006). In particular, *KCNQ2* A306T is associated with adult seizures in 16% of individuals who have this mutation (Ronen *et al.* 1993). These are the first orthologous mouse models of BFNC, and they display novel features consistent with the human disorder. Our results demonstrate that mice heterozygous for either mutation have reduced seizure thresholds, and homozygous adult knockin mice display spontaneous seizures into adulthood. Both reveal reduced amplitudes and increased deactivation kinetics of M-currents in the CA1 pyramidal cells of the hippocampus, a brain region likely to be involved in seizure generation in these models. Importantly, the homozygous knockin mice, despite the occurrence of many spontaneous seizures, do not exhibit either significant neuronal cell death or mossy fibre sprouting in the hippocampus. This lack of seizure-induced pathology probably contributes to the general sparing of cognitive deficits seen in patients with this M-current disorder.

Methods

Mice

Wild-type clones of *mKcnq2* and *mKcnq3* were isolated from a 129X1/Sv λ phage library (Stratagene) and subcloned into pBSk. The A306T point mutation in exon 6 of *mKcnq2* and the G311V point mutation in exon 5 of *mKcnq3* were introduced using standard PCR mutagenesis techniques. The ACN (Bunting *et al.* 1999) cassette was cloned into an *Xho*I site in intron 5 of *Kcnq2* and a *Sna*BI site in intron 6 of *Kcnq3* and these respective constructs were cloned into a thymidine kinase (TK) vector (Thomas & Capecchi, 1987). Within the ACN cassette the neomycin (neo) gene driven by the mouse RNA polymerase II promoter (polII) confers positive selection and TK gene confers negative selection of ES cells (Pluripotent embryo-derived stem cells). The targeting vector was linearized with *Not*I, introduced by electroporation into RI ES cells (Nagy *et al.* 1993) and selected for resistance to G418 and FIAU. Approximately 2×10^7 cells were electroporated and 71–82 colonies were isolated. DNA from each clone was isolated and analysed by standard Southern blotting techniques. Homologous recombination was verified using multiple restriction enzymes and probes to demonstrate the expected band shifts on Southern blot. ES cells from a single targeted clone were aggregated with C57BL/6-derived morulae, and implanted into a pseudopregnant C57BL/6 female. During chimeric male spermatogenesis, Cre recombinase driven by the murine angiotensin-converting enzyme promoter, tACE, confers loxP-mediated excision of the ACN cassette to yield a single remaining loxP site. Chimeric progeny were identified by coat colour and a single male was mated to C57BL/6J and FVB/NJ (Jackson labs) females for the generation of F1 offspring. F1 offspring were intercrossed to generate F2 experimental animals, and backcrossed five generations to produce N5 animals. Actual offspring ratios were compared to predicted Mendelian ratios using a Chi square test. A value of $P < 0.05$ was accepted as significant.

Genomic DNA obtained from tail biopsies of F1 and F2 animals was analysed for Cre-mediated self-excision of the ACN cassette and presence or absence of the respective mutation. Exon 6 of *Kcnq2* or exon 5 of *Kcnq3* was amplified by PCR primers located in the respective flanking intronic sequence and the PCR product was analysed by single strand conformational polymorphism analysis (SSCP) on a 20% acrylamide gel electrophoresed at 4°C. Under these conditions, each mutation produces a band shift with respect to wild-type. To verify self-excision, primers surrounding the remaining loxP site were used to amplify PCR products that were electrophoresed on a 2% agarose gel. The presence of a single loxP site verifies self-excision. Mouse colonies were maintained at the University of Utah in accordance with Institutional Animal Care and Use Committee approved protocols.

Chronic electroencephalographic (EEG) recordings

Adult homozygous N1F2 *Kcnq2* and *Kcnq3* mutant and littermate control mice (aged 3–6 months) on the C57BL/6 genetic background were implanted for chronic EEG recordings. Mice were anaesthetized with Avertin (1.25% tribromoethanol/amyl alcohol solution, I.P.) using a dose of 0.02 ml g^{-1}. Teflon-coated silver wire electrodes (0.005 in diameter) soldered to a microminiature connector were implanted bilaterally into the subdural space over frontal, central, parietal and occipital cortices. Digital EEG activity was monitored daily for up to 2 weeks during prolonged overnight and random 2 h sample recordings (Stellate Systems, Harmonie software version 5.0b). A video camera was used to monitor behaviour during the EEG recording periods. All recordings were carried out at least 24 h after surgery on mice freely moving in the test cage. Seizures without EEG monitoring were documented using iMovieHD software and a Canon camera.

Seizure threshold tests

B6;129-*Kcnq2*, B6;129-*Kcnq3* and FVB;129-*Kcnq3* F2 male mice, varying in age between 180 and 320 days, were used for the electroconvulsive threshold experiments. Minimal tonic hindlimb extension (THE) seizure testing (60 Hz, 0.2 ms sinusoidal current pulse, varying current intensities) was conducted with a stimulator previously described (Woodbury & Swinyard, 1952). Minimal THE seizures are characterized by a tonic–clonic flexion–extension sequence that starts with tonic forelimb extension, followed by hindlimb flexion, and terminates in full tonic hindlimb extension (180 deg to the torso) (White, 2002). All ECT testing was conducted between the hours of 1:00 and 5:00 p.m. to avoid confounding results that might arise from differences in circadian rhythm.

Seizure thresholds were tested using the staircase estimation procedure as previously described (Otto *et al.* 2004). Convulsive current (CC) curves were constructed and the CC value that produced a seizure in 50% of the mice tested (CC_{50}) and 95% confidence intervals (CI_{95}) were calculated. Statistical comparisons between wild-type and mutant mice were made by Probit analysis (Minitab 13). Significance was determined at $P < 0.05$.

Histology

Mice were deeply anaesthetized with Avertin (2.5% tribromoethanol/amyl alcohol solution, 0.8–0.9 ml per animal, I.P.) and perfused with 0.9% saline for 8 min. Brains were removed and cut at the sagittal midline. One-half was placed in formalin for 24 h followed by 70% ethanol. Brains were paraffin embedded and sliced at either 3 μm or 8 μm, mounted on slides, air-dried, deparaffinized using three changes of xylene for 5 min each and hydrated in graded alcohols (100%, 95% and 70%) or distilled water and stained as described below. The other half was frozen in isopentane–dry ice, and kept frozen at −80°C until stained with Timm. For Nissl stain, slides were stained with 0.5% Cresyl Echt Violet for 2 min, washed, dehydrated, cleared in xylene and coverslipped. For glial fibrillary acidic protein (GFAP) staining, the epitope is retrieved in citrate buffer pH 6.0 by microwave for 15 min at half power. Primary antibody diluted to 1 : 100 was incubated for 32 min at 40°C and secondary antibody (mouse Fab at 1 : 300, Dako) applied for 32 min. Detection was performed using the Enhanced Alkaline Phosphatase Red detection kit (Ventana) on the Ventana automated system at 40°C. Slides were counterstained with DAPI, washed, dehydrated and coverslipped. For NPY (Peninsula Laboratories), the epitope is retrieved in citrate buffer pH 6.0 by microwave for 15 min on half power, the primary antibody was incubated at 1 : 300 overnight at room temperature and the secondary antibody (rabbit 1 : 300, Sigma) was applied for 32 min. Detection was performed on the Ventana automated system at 40°C using the IView DAB detection kit followed by counterstaining with haematoxylin for 4 min.

For NeuN/TUNEL co-staining, epitope was retrieved in citrate buffer, pH 6.0 in an electric pressure cooker for 3 min, slides were placed in a Ventana autostainer at 40°C and incubated 1 : 100 for 32 min with NeuN antibody (Chemicon, Temecula, CA, USA) followed by a secondary antibody (Mouse Fab, Dako) at 1 : 300 for 32 min and detected with Enhanced Alkaline Phosphatase Red detection kit. Slides were then gently washed with dH_2O/Dawn (dishwashing liquid soap) and gently rinsed in dH_2O. Slides were treated with PBS for 1 min, Proteinase K (Dako Cytomation) 1 : 50 for 10 min at room temperature, rinsed in PBS for 5 min followed by the manufacturer's instructions from Chemicon ApopTag Plus Fluorescein In Situ Apoptosis Detection Kit. For non-fluorescent NeuN, the epitope was retrieved in an electric pressure cooker for 4 min. Primary antibody diluted to 1 : 100 was incubated for 32 min at 40°C and secondary antibody (mouse Fab at 1 : 200, Dako) applied for 32 min at 40°C. Detection was performed using the IView DAB detection kit. Slides were counterstained with haematoxylin for 4 min, washed, dehydrated and coverslipped.

For fluorojade-B (FJB; Histochem Inc., Jefferson, AR, USA) staining, slides were deparaffinized using Citrusolv, and pre-treated with 0.06% $KMnO_4$ for 15 min at room temperature. Slides were then incubated with 0.001% FJB in 0.1% acetic acid for 30 min at room temperature, washed with dH_2O and counterstained with DAPI, allowed to air dry and coverslipped. A positive control of either unperfused mouse brain slices (to detect red

blood cells) or a follicular lymphoma was included in every experiment.

For Timm staining, frozen brains were sectioned at 40 μm, mounted on slides, fixed with glutaraldehyde, sodium sulphide and calcium chloride, stained with silver nitrate (Sigma) in gum arabic, hydroquinone and citrate buffer and counterstained with cresyl violet. After washing, slides were dehydrated, cleared and coverslipped.

All pictures were taken on an Olympus IX70 microscope and control and treated images were adjusted for black and white levels using Adobe Photoshop.

Brain slice recordings

Brain slices were prepared from adult (8–10 weeks old) wild-type and mutant B6;129-*Kcnq2*, B6;129-*Kcnq3* and FVB;129-*Kcnq3* mice in a manner similar to previously described methods (Otto *et al.* 2006). Briefly, mice were anaesthetized with Nembutol (25 mg kg^{-1}, I.P.), decapitated, and their brains quickly removed and placed in oxygenated Ringer solution containing (mM): 200 sucrose, 26 $NaHCO_3$, 10 glucose, 3 KCl, 2 $MgSO_4$, 2 $CaCl_2$, 1.4 NaH_2PO_4. Brains were trimmed, mounted on a chuck, and 350 μm thick coronal slices were cut using a Vibratome slicer. Slices were then transferred to a holding chamber and allowed to incubate for $>$ 1 h in oxygenated Ringer solution similar to the above solution, but with 126 mM NaCl in place of sucrose. The NaCl Ringer solution pH was maintained at 7.37–7.40 with NaOH and continuous bubbling with 95% O_2–5% CO_2, and with an osmolarity of 305–310 mosmol l^{-1}.

Whole-cell perforated patch recordings were obtained from CA1 pyramidal neurons in the acute brain slice preparation using a MultiClamp 700A amplifier (Axon Instruments). Signals in voltage-clamp and current-clamp modes were acquired at 10 kHz, and filtered at 2 kHz for offline analysis using Clampfit 9. Glass capillaries (World Precision Instruments, Inc.) were pulled to 2.0–3.2 MΩ resistances using a micropipette electrode puller (Sutter Instrument Co.). Input and series resistance values of 80–120 MΩ and $<$ 15 MΩ, respectively, were used as selection criteria for accepting recordings and capacitance compensation was used. Amphotericin B (0.45–0.5 mg ml^{-1}) was dissolved in the intracellular solution containing (mM): 140 potassium gluconate, 10 Hepes, 10 KCl, and 0.2 $MgCl_2$ (pH adjusted to 7.28 with KOH; 290 mosmol l^{-1}). The external NaCl Ringer solution was supplemented with picrotoxin (50 μM) and NBQX (10 μM) to block $GABA_A$ receptor- and non-NMDA receptor-mediated responses, respectively (Otto *et al.* 2006).

In voltage-clamp mode, the M-type K^+ current ($I_{K(M)}$) amplitude was measured as the relaxation current in response to a voltage step protocol from −20 mV to return potentials of −40 mV, −50 mV, −60 mV and −70 mV, as previously described (Otto *et al.* 2006). $I_{K(M)}$ density was calculated as $I_{K(M)}$ amplitude (pA)/whole-cell capacitance (pF) for each cell. Kinetic analysis was performed by fitting the deactivation phase of the $I_{K(M)}$ trace with the standard single-component exponential fit equation: $f(t) = A_i\, e^{-t/\tau i} + C$. The y-axis was zeroed at the steady state for current deactivation at each hyperpolarizing step, and the fits were extrapolated to zero time. Although representative traces are shown in the figures, the amplitude measurements and the fits to the deactivation phase were performed on averaged traces (a minimum of five traces each).

Results

Generation of knockin mice

The targeting vectors consisted of the A306T point mutation in exon 6 of *Kcnq2* (Fig. 1*A*) or the G311V point mutation in exon 5 of *Kcnq3* (Fig. 1*B*) and the ACN self-excision cassette in the respective adjacent introns (Bunting *et al.* 1999). During chimeric male spermatogenesis, Cre recombinase driven by the murine testes specific angiotensin-converting enzyme promoter, tACE, confers loxP-mediated excision of the ACN cassette to yield a single remaining loxP site (third panel in Fig. 1*A* and *B*). Approximately 2×10^7 cells were electroporated and DNA from 70 to 80 colonies was analysed by standard Southern blotting techniques for targeted homologous recombination (Supplementary Fig. 1A and B). For each mutation a single male chimera was mated to C57BL/6J (B6) or FVB/NJ (FVB) females for the generation of B6;129 and FVB;129 F1 offspring, respectively. Genomic DNA obtained from tail biopsies was analysed for the presence or absence of the mutation and a single loxP site (Supplementary Fig. 1*C* and *D*). The FVB and B6 strains were chosen because of their wide variation in threshold to electrically induced seizures with increased susceptibility in the FVB background (Frankel *et al.* 2001). Mice were backcrossed and maintained as congenic strains and intercrossed at generations N1 and N5 for experiments. EEG recordings were performed on B6;129 N1F2 *Kcnq2* and *Kcnq3* mutant mice. Electrophysiological and seizure threshold experiments were performed on B6;129 N1F2 *Kcnq2* A306T mice and on both B6;129 and FVB;129 N1F2 mice carrying the *Kcnq3* G311V mutation. Due to unsuccessful breeding, FVB;129-*Kcnq2* mice were not available for the electrophysiology and seizure threshold experiments. Seizure video monitoring and histological experiments were performed on B6.129 and FVB.129 N5F2 littermate mice.

Mutant F2 mice on two genetic backgrounds were examined for ratios at birth and premature death and

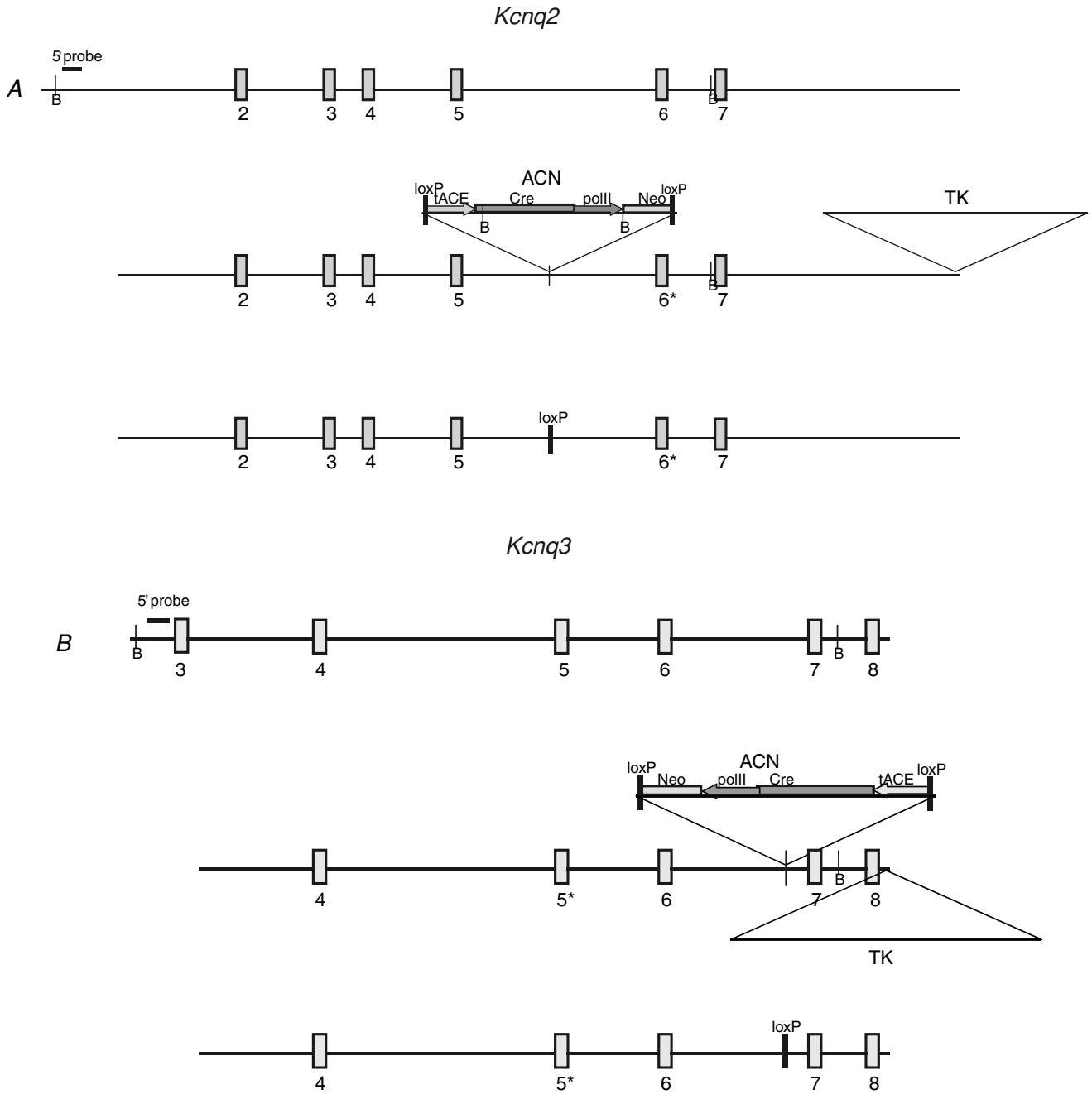

Figure 1. Generation of *Kcnq2* A306T and *Kcnq3* G311V knockin mice
SCHEMATIC representation of the wild-type and targeting construct used to make *Kcnq2*$^{A306T/A306T}$ (*A*) and *Kcnq3*$^{G311V/G311V}$ (*B*) mutant mice. Numbered boxes denote exons; the asterisk (*) represents the A306T missense change introduced into exon 6 of *Kcnq2* and G311V into exon 5 of *Kcnq3*; B denotes *Bam*H1 sites used in Southern blot analysis. The 5′ probe is used to confirm the presence of the endogenous and targeted alleles on genomic Southern blot of ES cells. The ACN cassette is made up of Cre-recombinase gene (*Cre*) driven by the testes-specific promoter from the angiotensin-converting enzyme gene (*tACE*); *Cre* is linked to the *Neo*^{r} selectable marker driven by the mouse RNA polymerase II large subunit gene (*polII*); the entire cassette is flanked by 34 bp loxP sites orientated in parallel. The HSV-TK (*TK*) gene is used for negative selection of ES cells. Following Cre-mediated self-excision in the chimeric mouse germline, a single loxP site and the point mutation remain (third panel in *A* and *B*).

significant deviation from expected Mendelian ratios were observed in most cases. The wild-type (B6.129-*Kcnq2*$^{+/+}$) : heterozygote (B6.129-*Kcnq2*$^{A306T/+}$) : homozygote (B6.129-*Kcnq2*$^{A306T/A306T}$) birth ratio of 1 : 2 : 0.6 ($P = 0.18$) for N1 and 1 : 2 : 0.4 ($P < 0.01$) for N5 was seen. For *Kcnq2* only N5 mice were successfully bred to the FVBN background strain and this FVB.129-*Kcnq2*$^{+/+}$: FVB.129-*Kcnq2*$^{A306T/+}$: FVB.129-*Kcnq2*$^{A306T/A306T}$ birth ratio was 1 : 2 : 0.1 ($P < 0.001$). N1 B6;129-*Kcnq3* mice were born in the ratio of 1 : 1.5 : 0.5 ($P < 0.01$) for wild-type : heterozygous : homozygous mutant. N5 B6.129-*Kcnq3* mice were born in a ratio of 1 : 1.3 : 0.2 ($P < 0.001$). N1 FVB;129-*Kcnq3* mice were born in the ratio of 1 : 1.5 : 0.4 ($P < 0.025$) for wild-type : heterozygous: homozygous mutant. N5 FVB.129-*Kcnq3* mice were born in ratios of 1 : 1.7 : 0.6 ($P = 0.05$). The body weight of N1F2 mice was normal for all genotypes whereas *Kcnq2*$^{A306T/A306T}$ and *Kcnq3*$^{G311V/G311V}$ mice in the N5F2 generation were considerably smaller than their heterozygous or wild-type littermates on both FVB and B6 background strains. This size difference was observed in both genders. For example, at weaning, male and female N5 B6.129 *Kcnq2*$^{A306T/A306T}$ mice were 22% to 46% smaller than their heterozygous or wild-type littermates. Due to a smaller body size, homozygous mutant mice were sometimes weaned a few days after normal sized littermates.

Both *Kcnq2* and *Kcnq3* homozygous mutant mice on either background strain died prematurely and a subset of these was observed by video monitoring to have died following seizures. The majority of FVB.129-*Kcnq2*$^{A306T/A306T}$ animals died from P16–P30 ($n = 13$). Survival curves demonstrate that most B6.129-*Kcnq2*$^{A306T/A306T}$ mice died during the first postnatal day or between P23 and P32 ($n = 27$, Fig. 2*A*). Survival curves for FVB.129-*Kcnq3*$^{G311V/G311V}$ animals showed that they died either at P0 or after P15 ($n = 28$,

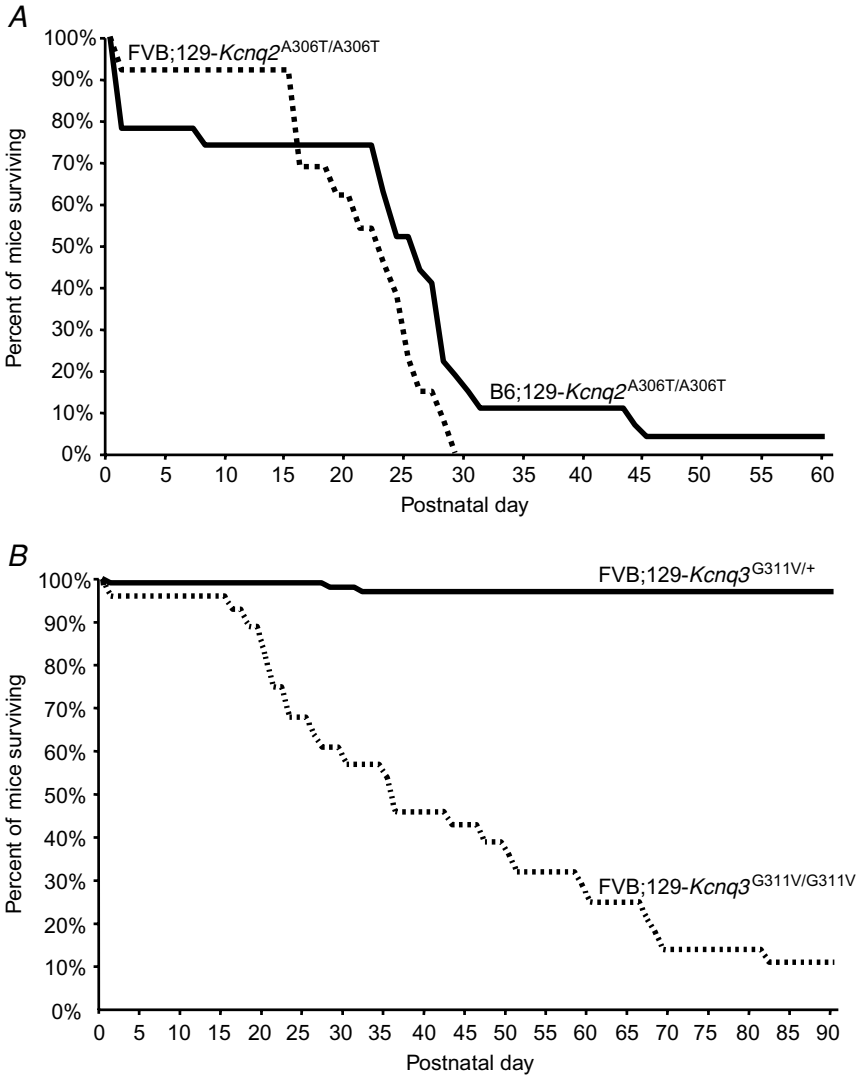

Figure 2. Survival curves of mutant mice
A, premature postnatal death as a result of the *Kcnq2* A306T knockin mutation. Survival curve shows that most N5F2 homozygous mutant mice on the FVB (dotted line, $n = 13$) and B6 (dark line, $n = 27$) genetic backgrounds died between P16 and P32. Heterozygous mutant mice did not die during the time frame described here. *B*, premature postnatal death as a result of the *Kcnq3* G311V knockin mutation. Survival curve shows that compared to heterozygous littermates (continuous line, $n = 84$), most N5F2 homozygous mutant mice on the FVB (dotted line, $n = 28$) genetic background died prematurely.

Fig. 2*B*), and 20% of these were observed to die during or immediately following a spontaneous seizure. In contrast to the majority of N5 FVB.129-*Kcnq3* mice, only 2/14 of N5 B6.129-*Kcnq3*$^{G311V/G311V}$ died prematurely, one immediately following birth and another of a severe seizure at P73. The remaining N5 B6.129-*Kcnq3*$^{G311V/G311V}$ mice were studied experimentally and thus could not be included in the survival analysis, although 70% of these animals survived at least to postnatal day 60.

Spontaneous seizures in *Kcnq2*$^{A306T/A306T}$ and *Kcnq3*$^{G311V/G311V}$ knockin mice on C57BL/6 and FVB/N backgrounds: EEG analysis and strain differences

B6;129-*Kcnq2*$^{A306T/A306T}$ and B6;129-*Kcnq3*$^{G311V/G311V}$ mice were implanted for prolonged video–EEG monitoring to characterize seizure patterns. Both homozygous mutations produce frequent generalized interictal cortical discharges (Fig. 3*A*). Figure 3*B* shows the EEG during a spontaneous generalized seizure in a B6;129-*Kcnq2*$^{A306T/A306T}$ mouse. In both mutants, behavioural signs of seizure activity precede the onset of abnormal synchronization and cortical epileptical discharges, and may outlast them, consistent with a subcortical seizure origin that secondarily generalizes (Videos 1 and 2 in the Supplementary data for Kcnq2 and Kcnq3, respectively). Automatisms, forepaw grooming and clonic twitching seen in both *Kcnq2* and *Kcnq3* knockin mice strongly suggest a limbic origin of the seizure.

To further characterize the seizure severity and frequency, N5 homozygous mutant mice on both the B6 and FVB genetic backgrounds were monitored by video although limited access of the camera did not permit prolonged monitoring of newborn pups in litters (Fig. 4*A*). All N5F2 B6.129-*Kcnq2*$^{A306T/A306T}$ mice monitored after weaning experienced at least one spontaneous generalized tonic clonic seizure of the forelimbs and hindlimbs

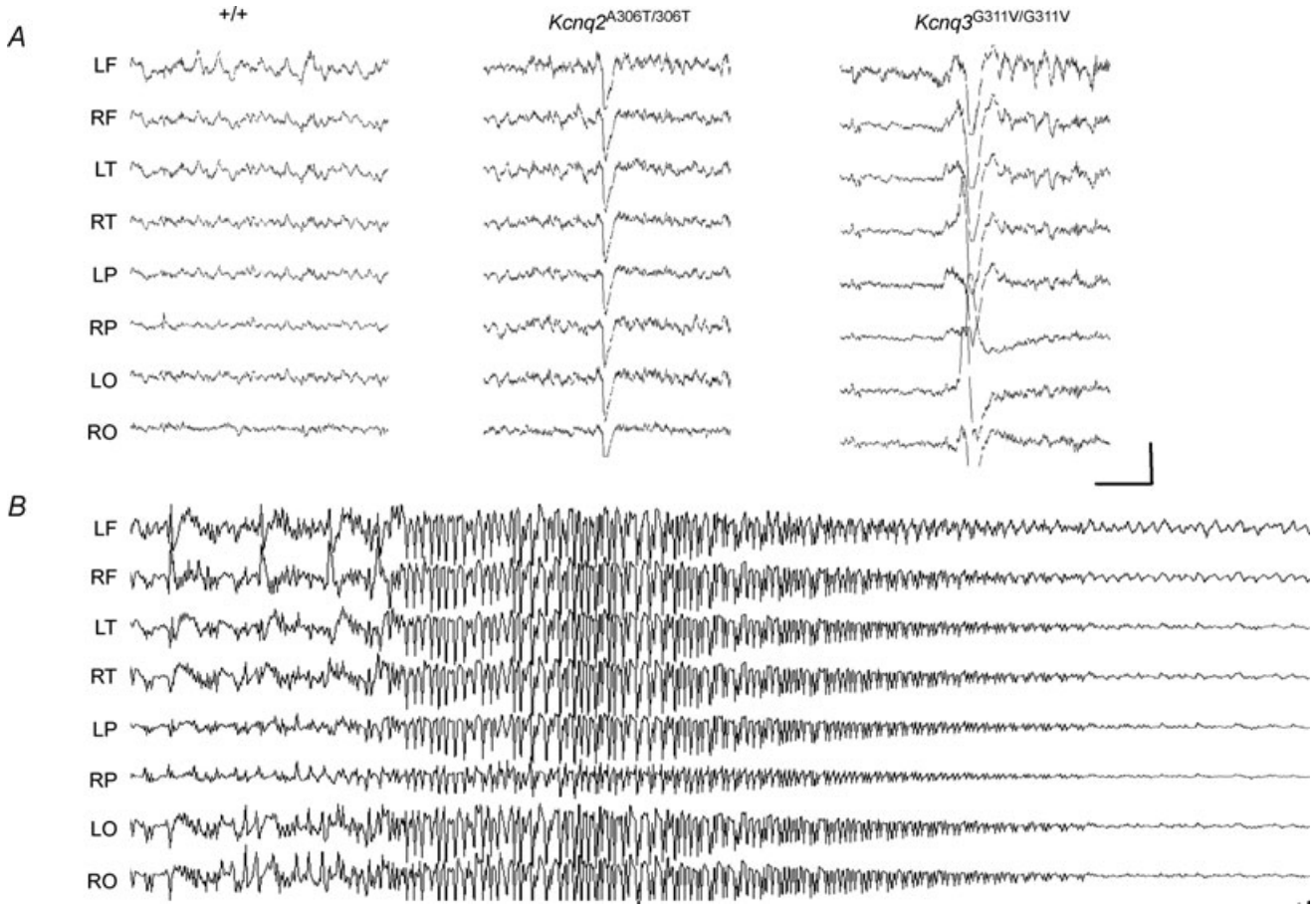

Figure 3. Seizure phenotypes of the *Kcnq2*$^{A306T/A306T}$ and *Kcnq3*$^{G311V/G311V}$ knockin mice
A, representative EEG from B6;129 +/+control, *Kcnq2*$^{A306T/A306T}$, and *Kcnq3*$^{G311V/G311V}$ knockin mice. Both homozygous mutations produce frequent generalized interictal cortical discharges. *B*, spontaneous generalized seizure in the *Kcnq2*$^{A306T/A306T}$ mouse. Electrode montage: left (L) and right (R) hemisphere, frontal (F), temporal (T), parietal (P), occipital (O). Calibration: 500 mV, 1 s.

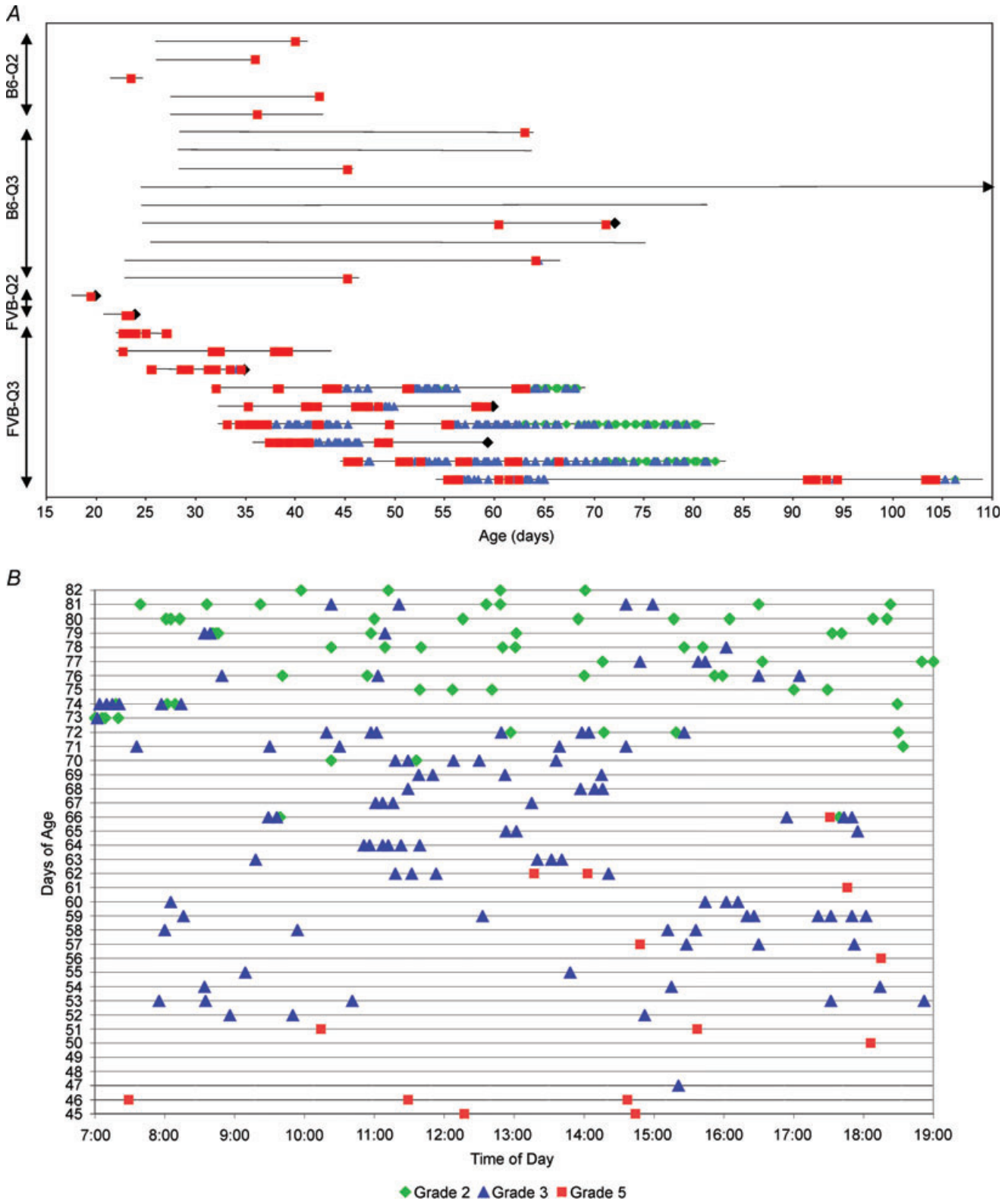

Figure 4. Behavioural seizures in homozygous mutant N5 mouse strains recorded by video after weaning

A, continuous 12 h daylight monitoring in four knockin homozygous mutant mice illustrating the dependence of seizure frequency and type on genetic background strain, mutation and age. B6-Q2 (B6.129-*Kcnq2*$^{A306T/A306T}$;

between the ages of P24 and P52 ($n = 7$). From onset to righting, the duration of seizures on this background was 1 : 04–2 : 55 min. Like mice on the B6 genetic background, N5F2 FVB.129-*Kcnq2*$^{A306T/A306T}$ mice monitored by video displayed an equally rapid onset spontaneous seizure in the second and third postnatal week but these seizures resulted in death in all cases (Video 3 in the Supplementary data).

The spontaneous behavioural seizure phenotype was monitored up to 120 days in N5 B6.129-*Kcnq3*$^{G311V/G311V}$ and N5 FVB.129-*Kcnq3*$^{G311V/G311V}$ mice for frequency and severity. Spontaneous seizures were observed as early as the second postnatal week in FVB.129-*Kcnq3*$^{G311V/G311V}$ mice. After weaning, FVB.129-*Kcnq3*$^{G311V/G311V}$ mutant animals experienced multiple spontaneous recurrent seizures on a near-daily basis. An example of one such animal monitored from P45 to P82 during the light cycle is shown in Fig. 4*B*. We developed our own seizure grading scale, grades one to five, because it describes our seizure phenotype more precisely than the commonly used Racine scale that describes the slightly different behavioural stages of seizures during the 'kindling' procedure in rats (Michalakis *et al.* 1998). A comparison of our scale to the Racine scale is presented in Supplementary Table 1. Data from multiple animals showed at P30–P45, seizure severity declined from almost daily grade 5 (forelimb and hindlimb tonic extension; Supplementary Video 4) seizures to less severe grade 3 (forelimb and hindlimb clonus only; $n = 6$; see Supplementary Video 5) seizures and by P65–P75, mice showed primarily grade 2 (bilateral forelimb clonus, orofacial automatisms, jaw chomping, head clonus, occasional falling and rearing; $n = 4$) seizures. Grade 4 (forelimb tonic extension and hindlimb clonus) and grade 1 (rapid running) were rarely observed. In addition to a decline in severity, they also showed a higher frequency of seizures that clustered with increasing age. Clustering consists of multiple grade 2 or 3 seizures occurring 1 to 5 min apart, separated by alert conscious behaviour. In cases where animals did not have generalized seizures for longer than 48 h, the breakthrough seizure was a grade 5. Long-term monitoring beyond P120 was not done because almost all animals eventually died of seizures or what appeared to be seizure-related complications. No gender differences in seizure behaviour were observed, consistent with the human BFNC phenotype. In contrast to FVB.129-*Kcnq3*$^{G311V/G311V}$ mice that all experienced recurrent seizures, B6.129-*Kcnq3*$^{G311V/G311V}$ mice exhibited only rare spontaneous seizures. About half of the B6.129-*Kcnq3*$^{G311V/G311V}$ animals experienced a single grade 5 seizure between weaning and postnatal day 72.

Seizure thresholds are decreased in older *Kcnq2*$^{A306T/+}$ and *Kcnq3*$^{G311V/+}$ heterozygotes

Since 16% of individuals with neonatal-onset BFNC experience a seizure later in life, we measured the seizure susceptibility of older heterozygous (P140–P382) mice to test the hypothesis that these mice may have reduced electroconvulsive seizure thresholds (Otto *et al.* 2004). Convulsive current (CC) levels at which 50% of mice were predicted to seize (CC_{50}) and corresponding 95% confidence intervals (CI_{95}) were calculated for the tonic hindlimb extension seizure.

The calculated CC curve for male B6;129-*Kcnq2*$^{A306T/+}$ heterozygous mice and their littermate controls are shown in Fig. 5*A*. The CC_{50} value for this type of seizure was significantly lower for the *Kcnq2*$^{A306T/+}$ mice (9.6 mA) than for the wild-type control mice (11.7 mA) ($P = 0.027$) indicating that the mutant mice had a reduced seizure threshold. The calculated CC curves for male B6;129-*Kcnq3*$^{G311V/+}$ and FVB;129-*Kcnq3*$^{G311V/+}$ mice and their littermate controls shown in Fig. 5*B* and *C* demonstrate a reduced seizure threshold in the mutant mice on both genetic inbred backgrounds. The CC_{50} value for this seizure type was significantly lower for the B6;129-*Kcnq3*$^{G311V/+}$ mice (11.6 mA) than for the wild-type control mice (13.6 mA) ($P = 0.046$) and also for FVB;129-*Kcnq3*$^{G311V/+}$ mice when compared to the wild-type control mice (7.0 mA *versus* 8.8 mA, $P = 0.012$). Interestingly, the seizure thresholds for the wild-type FVB mice were also lower than the seizure thresholds for the B6 wild-type mice, consistent with a previous report on the importance of genetic background on seizure susceptibility (Frankel *et al.* 2001).

$n = 5$; at least one stage 5 seizure per animal), B6-Q3 (B6.129-*Kcnq3*$^{G311V/G311V}$; $n = 9$; 4 out of 9 animals experienced no seizures during the monitoring period), FVB-Q2 (FVB.129-*Kcnq2*$^{A306T/A306T}$; $n = 2$, most animals die of presumed seizures between P16 and P30) and FVB-Q3 (FVB.129-*Kcnq3*$^{G311V/G311V}$; $n = 9$; see Supplemental Table 1 for detailed seizure number). Horizontal black lines correspond to monitoring period for each mouse; black diamond, animals died during or immediately after seizure; arrow, mouse was monitored until P116. *B*, during the 12 h light cycle, a typical FVB.129-*Kcnq3*$^{G311V/G311V}$ knockin mouse experienced spontaneous generalized seizures that went from almost daily grade 5 (forelimb and hindlimb tonic extension) seizures around P30–P45 to primarily grade 3 (forelimb and hindlimb clonus) seizures to primarily grade 2 (bilateral forelimb clonus, orofacial automatisms, jaw chomping, head clonus, occasional falling and rearing) seizures at P65–P75.

Normal hippocampal morphology in *Kcnq2*$^{A306T/A306T}$ mice following at least one spontaneous seizure

To examine whether seizures in *Kcnq2* knockin mice are accompanied by alterations in hippocampal morphology, we performed histology on the hippocampi of N5 B6.129 *Kcnq2*$^{A306T/A306T}$ mice ($n = 6$) that exhibited at least one documented generalized tonic–clonic seizure. Since the majority of N5 *Kcnq2* mutant mice on the FVB/N genetic background died immediately following seizures they could not be perfused for the histology experiments. Nissl-stained coronal sections from knockin mice did not exhibit pyknotic cells in any of the pyramidal and dentate granule cell layers of the hippocampus, suggesting an absence of cell death on this genetic background during the postnatal period. An example is shown in Fig. 6*A* and *B* from a 42-day-old control mouse and homozygous mutant mouse killed 18 h after a generalized tonic clonic seizure that lasted 2 min and 55 s. Staining of the hippocampal interneurons and principal cells with NeuN, a neuronal marker, did not appear to significantly differ between homozygous knockin and wild-type mice (Fig. 6*C* and *D*). Staining of adjacent sections with TUNEL and fluorojade-B (FJB) for cell death was also negative (data not shown). Along with cell death, an up-regulation of neuropeptide Y (NPY) in the mossy fibre pathway is a well-documented compensatory response to seizures induced by genetic or pharmacological manipulation (Scharfman & Gray, 2006). Thirty-nine hours after the last seizure, a 41-day-old B6.129 *Kcnq2*$^{A306T/A306T}$ mouse exhibits an increase in the expression of NPY in the mossy fibre axons that project from the dentate granule cells to the stratum lucidum (Fig. 6*E* and *F*). This up-regulation was observed in four homozygous mutant mice after documented seizures at P24, P36, P36 and P41. An up-regulation of NPY was not seen in a P30 B6.129 *Kcnq2*$^{A306T/A306T}$ homozygous mutant mouse that did not show spontaneous seizure activity when monitored after weaning (Supplementary Fig. 2*A*).

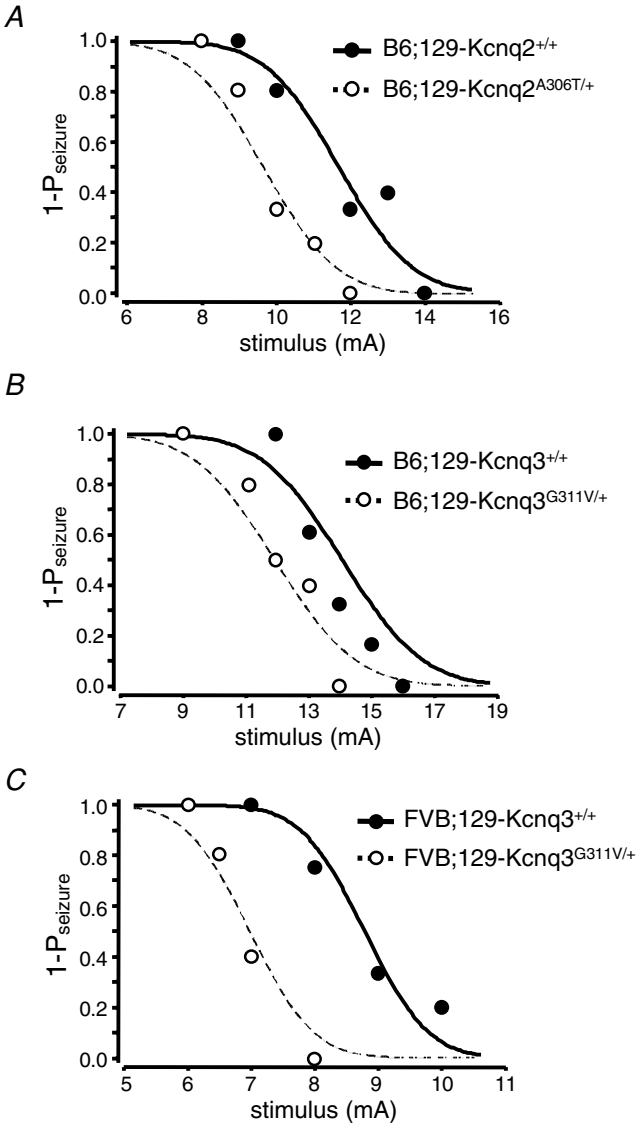

Figure 5. *Kcnq2*$^{A306T/+}$ and *Kcnq3*$^{G311V/+}$ mice exhibit reduced thresholds to electroconvulsive seizures
Convulsive current curves generated from electroconvulsive threshold (ECT) testing in male B6;129-*Kcnq2*$^{A306T/+}$ (*A*), male B6;129-*Kcnq3*$^{G311V/+}$ (*B*) and male FVB;129-*Kcnq3*$^{G311V/+}$ (*C*) *versus* littermate control mice. These curves show that the *Kcnq2* A306T mutation on the B6 inbred background and the *Kcnq3* G311V mutation on both background strains resulted in a significant reduction in seizure threshold to tonic hindlimb extension seizures ($P < 0.05$). Convulsive current data are expressed in terms of 1-;seizure probability (1-$P_{seizure}$). •, B6;129-*Kcnq2*$^{+/+}$ (*A*), B6;129-*Kcnq3*$^{+/+}$ (*B*) and FVB;129-*Kcnq3*$^{+/+}$mice (*C*); and ○, B6;129-*Kcnq2*$^{A306T/+}$ (*A*), B6;129-*Kcnq3*$^{G311V/+}$ (*B*) and FVB;129-*Kcnq3*$^{G311V/+}$ mutant mice (*C*) represent individual data points used to construct the curves, which are indicated by continuous and dotted lines, respectively.

Histological analysis of *Kcnq3*$^{G311V/G311V}$ knockin mice following recurrent seizures

In order to identify neuropathological evidence of hyperexcitability as a result of recurrent seizures, N5 FVB.129-*Kcnq3*$^{G311V/G311V}$ mice were examined for markers of chronic excitability: neuropeptide Y up-regulation, glial proliferation, neuronal loss and mossy fibre sprouting, and compared to their littermate controls or animals matched within 1 week of age. NPY was up-regulated in all homozygous mutant mice ($n = 11$) examined past P29. Examples are shown at P30 (Fig. 7*B*) and P90 (Fig. 7*C*) compared to a P30 wild-type mouse in Fig. 7*A*. No up-regulation of NPY was seen in P8, P11 and P14 homozygous mutant mice (Supplemental Fig. 2*B*). FVB.129-*Kcnq3*$^{G311V/G311V}$ mice at ages ranging from P30 to P120 ($n = 13$) exhibited a noticeable increase in glial fibrillary acidic protein (GFAP) staining without an increase in nuclear DAPI staining. Examples from a P34

and a P120 mouse are shown in Fig. 7*E* and *F* compared to P103 heterozygote mouse (Fig. 7*D*).

Since many animal models that develop spontaneous recurrent seizures exhibit a marked loss of hilar interneurons and pyramidal CA1 neurons, we used the TUNEL stain to look for apoptotic cell death and FJB for necrotic cell death. No evidence of apoptotic neuronal loss in the hippocampus was found (data not shown) and co-labelling of NeuN with TUNEL revealed intact pyramidal and dentate granule cell layers. NeuN staining also showed a comparable number of hippocampal interneurons in the hilar and stratum lacunosum moleculare (arrows) regions in P29 and P120 FVB.129-*Kcnq3*$^{G311V/G311V}$ mice (Fig. 7*H* and *I*) despite the marked difference in seizure number between these two ages. FJB staining did not reproducibly label hippocampal cells in P29 homozygous mutant mice (Fig. 7*K*; inset represents hippocampal layer). At multiple later time points up to P120 ($n = 6$), there was a clear absence of FJB staining in the principal neurons of the hippocampal formation. However, a reproducible staining of cells of undetermined origin in the dentate subgranular zone indicates select regions of necrosis in the hippocampus after recurrent seizures (Fig. 7*L*; inset represents hippocampal layer).

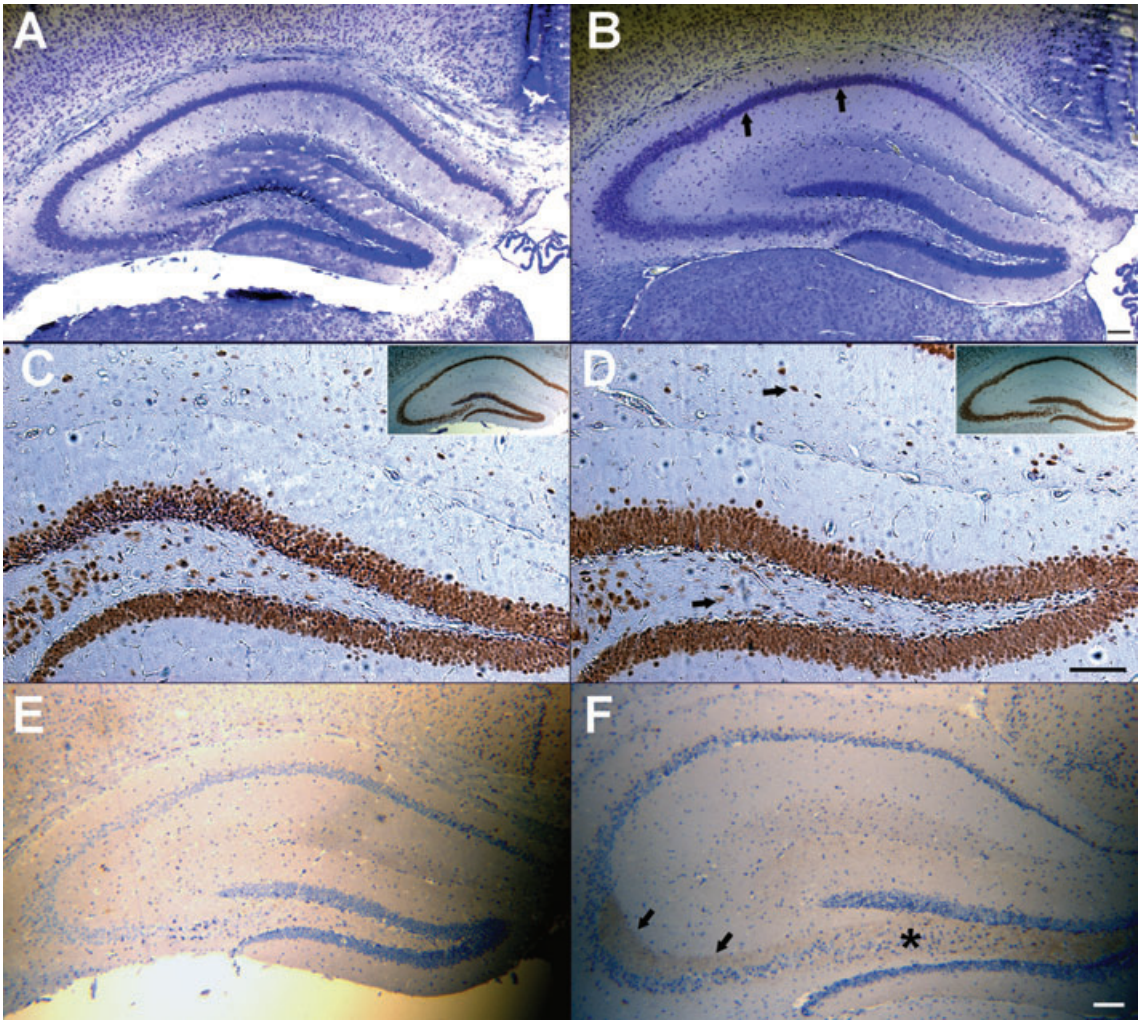

Figure 6. Histological analysis of hippocampi of seizure positive B6.129-*Kcnq2*$^{A306T/A306T}$ knockin mice
Nissl-stained coronal sections through the hippocampus of P42 aged B6.129-*Kcnq2*$^{+/+}$ (*A*) and B6.129-*Kcnq2*$^{A306T/A306T}$ littermates (*B*) showing a lack of punctate staining in the CA1 pyramidal cell layer (arrows). Adjacent coronal Neu-N stained sections showing comparable hilar and stratum lacunosum interneurons (arrows) in B6.129-*Kcnq2*$^{+/+}$ (*C*) and B6.129-*Kcnq2*$^{A306T/A306T}$ (*D*) mice. Insets illustrate the corresponding hippocampal section from which *C* and *D* were taken. Induction of NPY in hilar (*) and stratum lucidum (arrows) mossy fibres of *Kcnq2*$^{A306T/A306T}$ mice (*F*) following at least one generalized tonic–clonic seizure not seen in an age-matched control mouse (*E*). *E* and *F* are counterstained with haematoxylin. Scale bars, 100 μm.

Since spontaneous recurrent seizures of temporal lobe origin are often accompanied by synaptic reorganization of the axons of the dentate granule cells, we examined the mossy fibres in the inner molecular layer using the Timm stain to label their zinc content. Timm staining in FVB.129-*Kcnq3*$^{G311V/G311V}$ mice from P33–P120 ($n = 10$) did not show the presence of mossy fibre sprouting into the inner molecular layer of the dentate gyrus, consistent with the absence of principal hippocampal cell loss. An example of a 108-day-old FVB.129-*Kcnq3*$^{G311V/G311V}$ mouse is shown in Fig. 7*N* and *O* compared to a littermate wild-type mouse (Fig. 7*M*).

Effects of *Kcnq2* S6 transmembrane domain mutation and the *Kcnq3* pore mutation on $I_{K(M)}$ amplitude, density and deactivation kinetics in CA1 neurons

We evaluated the effects of the *Kcnq2* and *Kcnq3* mutations that cause BFNC in patients on $I_{K(M)}$ function in CA1 pyramidal cells of the hippocampus. While $I_{K(M)}$ is expressed in many different cell types throughout the brain, these neurons were chosen for study for several reasons. First, Kcnq2 and Kcnq3 mRNA and protein are expressed abundantly in these cells (Shah *et al.* 2002; Devaux *et al.* 2004); second, the hippocampus is directly implicated in limbic epilepsy, and finally, $I_{K(M)}$ has been extensively studied in this cell type in normal and other animal models of *Kcnq2* mutations (Peters *et al.* 2005; Otto *et al.* 2006). Hippocampal CA1 neurons in brain slices prepared from wild-type (*Kcnq2*$^{+/+}$), heterozygous (*Kcnq2*$^{A306T/+}$) and homozygous (*Kcnq2*$^{A306T/A306T}$) B6;129 knockin mice exhibited an $I_{K(M)}$ across a range of hyperpolarizing return steps (Fig. 8*A*; $n = 5$–14 cells per genotype per return step). This voltage protocol results in the slow and measurable deactivation of the M-current. Previous work has demonstrated that this current is blocked by the M-channel blockers linopirdine and TEA in wild-type B6 mice suggesting that there is little contamination from I_H under these recording conditions (Otto *et al.* 2006). CA1 neuronal $I_{K(M)}$ amplitudes from *Kcnq2*$^{A306T/+}$ mice were no different than those measured in *Kcnq2*$^{+/+}$ mice but were significantly decreased in *Kcnq2*$^{A306T/A306T}$ mice at every return step tested (Fig. 8*B*). Since a decrease in current amplitude could be explained by a decrease in CA1 neuron size, whole-cell capacitance, a relative approximation of cellular surface area, was used to convert amplitudes to current densities. As was the case with the current amplitude results, $I_{K(M)}$ density was not significantly affected in *Kcnq2*$^{A306T/+}$ CA1 neurons, but was decreased in *Kcnq2*$^{A306T/A306T}$ CA1 neurons at all voltages (Fig. 8*C*).

The time constant of deactivation of the $I_{K(M)}$ currents was evaluated by fitting a single exponential to the decay phase of the current. When compared to the currents recorded in CA1 neurons in brain slices obtained from *Kcnq2*$^{+/+}$ mice, the deactivation of $I_{K(M)}$ is significantly accelerated in *Kcnq2*$^{A306T/+}$ CA1 neurons at the −60 and −50 mV return steps (Fig. 8*D*). Deactivation kinetics are also accelerated in *Kcnq2*$^{A306T/A306T}$ CA1 neurons at the −70 and −60 mV return steps (Fig. 8*D*), but at −50 and −40 mV, deactivation could not be adequately fitted with a standard exponential decay equation and thus the time constants at these voltages are not plotted.

In brain slices prepared from B6;129-*Kcnq3*$^{+/+}$, B6;129-*Kcnq3*$^{G311V/+}$ and B6;129-*Kcnq3*$^{G311V/G311V}$ knockin mice, CA1 neurons exhibited a measurable $I_{K(M)}$ evoked by a range of hyperpolarizing return steps (Fig. 9*A*; $n = 8$–21 cells per genotype per return step). In hippocampal CA1 neurons in brain slices prepared from B6;129-*Kcnq3*$^{G311V/+}$ mice, $I_{K(M)}$ amplitudes were no different from those measured in B6;129-*Kcnq3*$^{+/+}$ slices (Fig. 9*B*). However, in B6;129-*Kcnq3*$^{G311V/G311V}$ CA1 neurons, $I_{K(M)}$ amplitude was significantly decreased at every return voltage step tested. $I_{K(M)}$ density, derived from $I_{K(M)}$ amplitude values divided by membrane capacitance, was significantly decreased in B6;129-*Kcnq3*$^{G311V/+}$ CA1 neurons only at the −50 mV step, but was decreased in B6;129-*Kcnq3*$^{G311V/G311V}$ CA1 neurons at all return steps (Fig. 9*C*). Deactivation kinetics were also examined in these recordings. The time constant of deactivation is faster in B6;129-*Kcnq3*$^{G311V/+}$ CA1 neurons only at the −60 mV return step (Fig. 9*D*), while B6;129-*Kcnq3*$^{G311V/G311V}$ deactivation is only accelerated at the −70 mV return step. $I_{K(M)}$ deactivation in B6.129-*Kcnq3*$^{G311V/G311V}$ CA1 neurons was too linear to be adequately fitted with a standard exponential decay equation at potentials above −60 mV (data not shown).

In brain slices prepared from *Kcnq3* mice on the inbred FVB background, CA1 neurons exhibited an $I_{K(M)}$ across a range of hyperpolarizing return steps (Fig. 9*E*; $n = 5$–9 cells per genotype per return step). In hippocampal CA1 neurons in brain slices prepared from FVB;129-*Kcnq3*$^{G311V/+}$ mice, $I_{K(M)}$ amplitudes were no different from those measured in FVB;129-*Kcnq3*$^{+/+}$ slices (Fig. 9*F*). However, in FVB;129-*Kcnq3*$^{G311V/G311V}$ CA1 neurons, $I_{K(M)}$ amplitude was significantly decreased at the −60, −50 and −40 mV return steps. $I_{K(M)}$ density was not affected in FVB;129-*Kcnq3*$^{G311V/+}$ CA1 neurons, but was significantly decreased in FVB;129-*Kcnq3*$^{G311V/G311V}$ CA1 neurons at all return steps (Fig. 9*G*). Deactivation of $I_{K(M)}$ in FVB;129-*Kcnq3*$^{G311V/+}$ CA1 neurons was not significantly affected at any return step (Fig. 9*H*), while FVB;129-*Kcnq3*$^{G311V/G311V}$ deactivation kinetics are accelerated at every step in which they could be adequately fit with a single exponential.

Intrinsic membrane properties were examined in CA1 pyramidal neurons from all mutant mice.

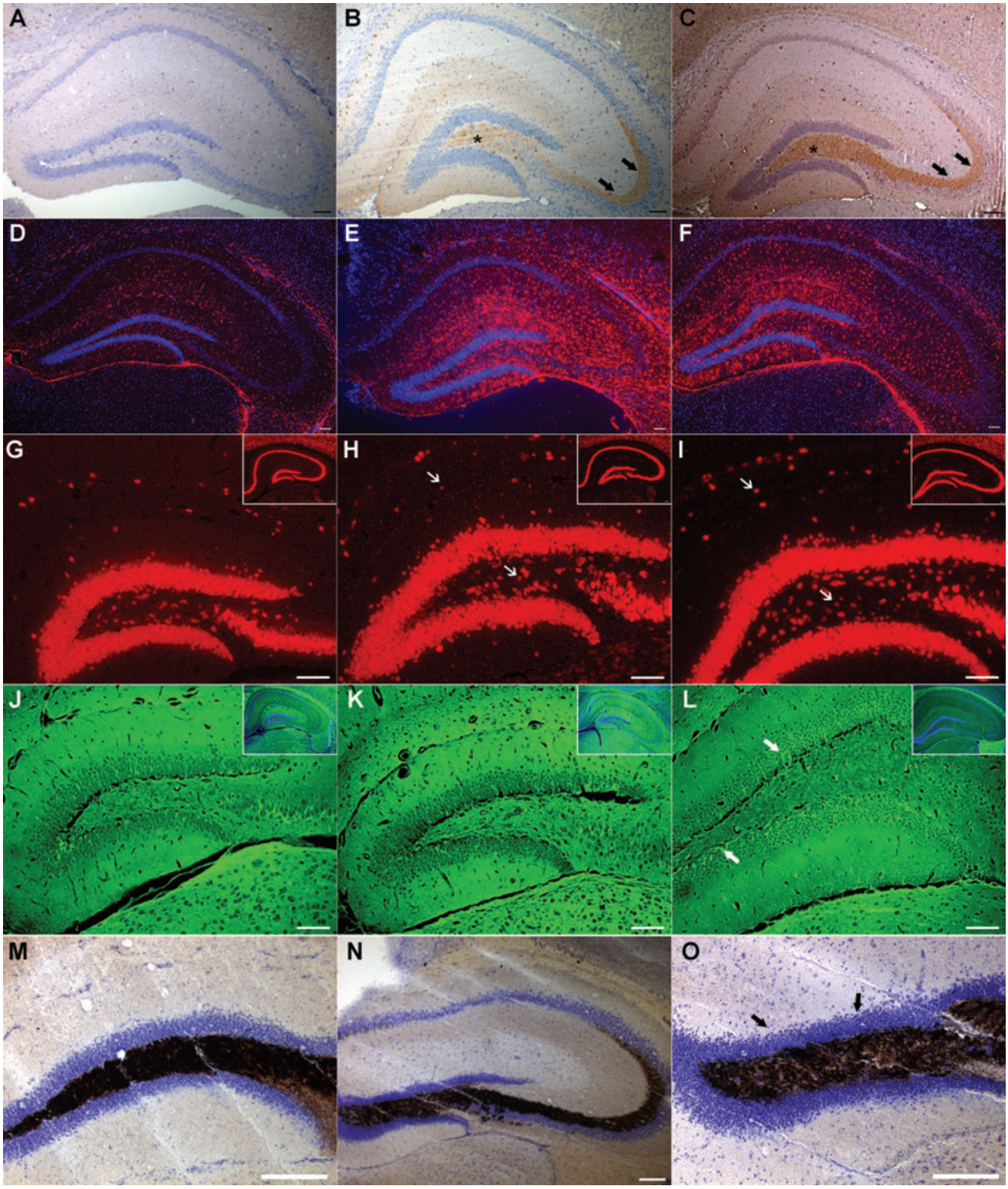

Figure 7. Hippocampal morphology of young P29–P34 and older P90–P120 FVB.129-*Kcnq3*$^{G311V/G311V}$ mice and representative controls

Up-regulation of NPY in the hilar (*) and stratum lucidum (arrows) mossy fibres of P30 (*B*) and P90 (*C*) mice. GFAP staining shows astrogliosis in multiple hippocampal regions of P34 (*E*) and P120 (*F*) FVB.129-*Kcnq3*$^{G311V/G311V}$ mice. NeuN staining shows normal hippocampal CA1 (insets) neuronal and hilar and stratum lacunosum moleculare

Neither the *Kcnq2* A306T mutation nor the *Kcnq3* G311V mutation significantly alters input resistance, series resistance, resting membrane potential or membrane capacitance of CA1 neurons. These data are available online (Supplementary Tables S3, S4 and S5).

Discussion

We have successfully knocked in the precise disease-causing mutations into the S6 transmembrane domain of the *Kcnq2* gene and the pore of the *Kcnq3* gene in order to study the salient features of the inherited childhood disorder of BFNC. To our knowledge, the *Kcnq3* G311V knockin mouse is the first mouse model to be reported with a KCNQ3 defect. Unlike previously described *Kcnq2* knockout mutant mice, both knockin mouse strains survive and, interestingly, develop spontaneous seizures lasting into adulthood. The seizures were behaviourally manifest during the second postnatal week and may have begun during the neonatal period; however, we were technically unable to routinely monitor video–EEG seizure activity during the first 2 weeks of life. This leaves open the possibility that those mice that do not appear to experience recurrent seizures after weaning, may have experienced neonatal seizures that remit in early postnatal development as often occurs in the human disorder. Remission might also occur in knockin mice if they are bred onto a different genetic background strain. Nonetheless, we have found that older heterozygous mutant mice have reduced thresholds to electrically induced seizures, supporting the hypothesis that these mutations confer enhanced seizure susceptibility into adulthood. This finding is important as 16% of BFNC individuals, and in particular those bearing the *KCNQ2* A306T mutation, will display epilepsy later in life (Ronen *et al.* 1993). This rate is considerably higher than the 1% epilepsy incidence of the general population. In addition to seizures, both potassium channel gene mutants exhibited reduced M-channel current amplitude and density and faster deactivation kinetics in hippocampal pyramidal neurons. The decrease in induced seizure threshold without changes in current amplitude in the heterozygous knockin mice may be due, at least in some cases, to the faster deactivation kinetics that were observed in $I_{K(M)}$ currents recorded from heterozygous mice. Finally, our results demonstrate that even after experiencing hundreds of spontaneous seizures, *Kcnq3* mice on the FVB genetic background lack evidence of the more deleterious forms of synaptic plasticity, such as granule cell mossy fibre reorganization or hippocampal neuronal loss. Although no analysis of hippocampal pathology is available for the human BFNC cases, this benign pathological picture is consistent with the preserved cognition and learning in patients who harbour this specific mutation (Ryan *et al.* 1991).

In the homozygous mutant mice that carry specific disease-causing *Kcnq2* and *Kcnq3* mutations, a significant suppression of the M-current in CA1 neurons is accompanied by robust spontaneous seizures. Indeed, in voltage steps to −40 mV, the reduction in $I_{K(M)}$ ranged from 38 to 46%, depending on the mutation and the background strain. The hypothesis that hypofunctional M-channels serve as the initial trigger which probably sets up the foundation for the epileptic network has been previously proposed in response to results from earlier studies performed in expression systems and electrophysiology studies (Schroeder *et al.* 1998; Chung *et al.* 2006). Both the A306T and G311V mutations show a 20–40% decrease in the amplitude of currents in the *Xenopus* oocyte expression system (Schroeder *et al.* 1998), and Chung *et al.* have demonstrated a 50–75% reduction in axonal surface expression of these transfected mutant subunits in cultured hippocampal neurons (Chung *et al.* 2006). This is consistent with our findings that there is a significant voltage-dependent reduction in current amplitude and density in CA1 neurons in mice homozygous for these mutations (see Figs 8 and 9). It is currently not clear why deactivation kinetics are altered in CA1 neurons in mice with these mutations or why $I_{K(M)}$ amplitude is for the most part unaffected in mice heterozygous for the mutations. However, heterologous expression systems notably lack many auxiliary proteins and signal transduction cascades that may play a role in M-current function. In addition compensatory processes with respect to expression of other Kcnq subunits could occur over the course of development in mice heterozygous for the mutations examined here. The results of the

(arrows) interneuronal layers in P29 (*H*, inset lower magnification) and P120 (*I*, inset lower magnification) FVB.129-*Kcnq3*$^{G311V/G311V}$ mice. Fluorojade staining of hippocampal layers shows no reproducible neuronal cell death in P29 (*K*) and P120 (*L*) FVB.129-*Kcnq3*$^{G311V/G311V}$ mice, except cells (*L*, arrows) stained in the dentate granule proliferative zone in the P120 mutant mouse. The insets are a lower magnification with the same FJB stained sections counterstained with DAPI illustrating the hippocampal level analysed. Timm staining of a P108 mutant mouse showing normal mossy fibre staining in the dentate gyrus and stratum lucidum (*N*) and a lack of staining in the inner molecular layer (*O*) (arrows). Scale bars, 100 μm.

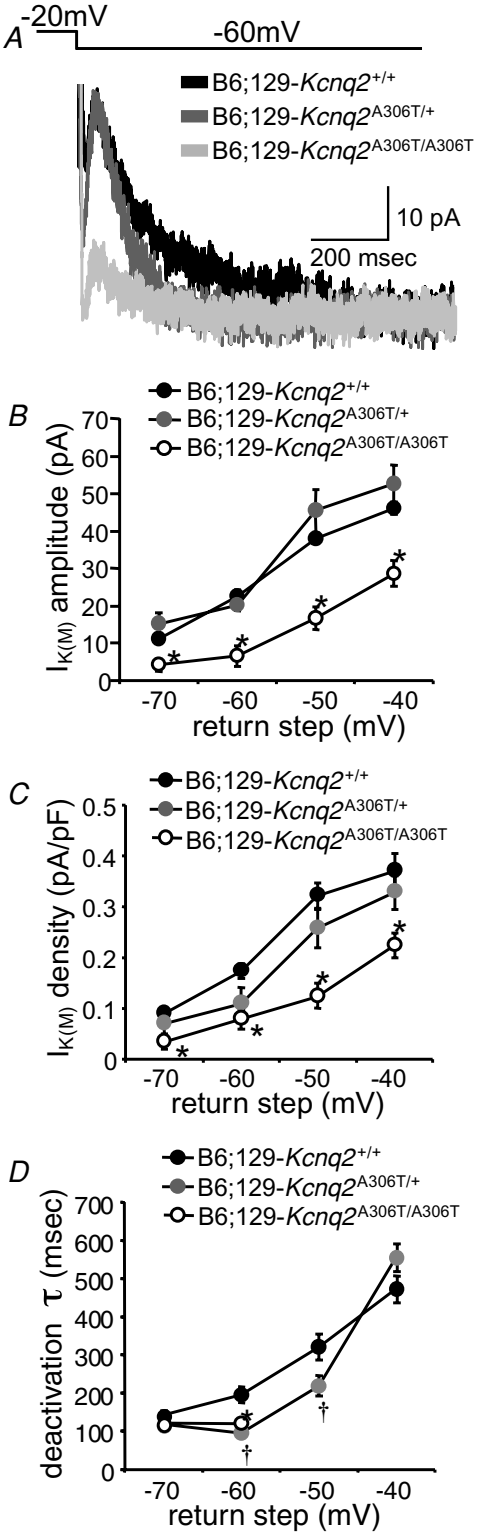

Figure 8. $I_{K(M)}$ amplitude and density are decreased in B6;129 CA1 neurons carrying the *Kcnq2* A306T mutation
A, sample traces recorded from wild-type B6;129-*Kcnq2*$^{+/+}$ (black), heterozygous mutant B6;129-*Kcnq2*$^{A306T/+}$ (darker grey), and homozygous mutant B6;129- *Kcnq2*$^{A306T/A306T}$ (lighter grey) CA1 neurons in response to the −20 to −60 mV step. $I_{K(M)}$ amplitude is measured from the deactivation hump (10–20 ms after the hyperpolarizing step) to the steady-state level at the end of the trace. *B*, $I_{K(M)}$ amplitude is decreased relative to wild-type in B6;129-*Kcnq2*$^{A306T/A306T}$ CA1 neurons (*$P < 0.001$; all return steps). *C*, $I_{K(M)}$ density is also decreased in B6;129- *Kcnq2*$^{A306T/A306T}$ CA1 neurons (*$P < 0.005$; all return steps). *D*, $I_{K(M)}$ deactivation kinetics are faster in B6;129-*Kcnq2*$^{A306T/+}$ CA1 neurons than wild-type at the −60 and −50 mV return step (†$P < 0.05$); in B6;129-*Kcnq2*$^{A306T/A306T}$ CA1 neurons, $I_{K(M)}$ deactivation is faster than wild-type at the −60 mV step (*$P < 0.05$).

present investigation directly establish that mutations causing human BFNC do indeed precipitate either decreased $I_{K(M)}$ amplitude, density or accelerated deactivation kinetics in CA1 neurons of the hippocampus. Pharmacological block of M-channels in hippocampal neurons enhances spike afterdepolarization and induces intrinsic bursting, two important parameters that normally serve to stabilize neuronal firing (Yue & Yaari, 2004). Similarly, CA1 neurons in the *Kcnq2* C-terminal deleted Szt1 mouse have a decreased M-current, a reduction in spike frequency adaptation and a subsequent increase in action potential frequency (Otto *et al.* 2006). In another transgenic mouse model with seizures, suppression of the M-current attenuated the medium afterhyperpolarization and reduced the intrinsic subthreshold theta resonance of CA1 pyramidal neurons (Peters *et al.* 2005). Future work with these novel BFNC mouse models may help to further elucidate the role of $I_{K(M)}$ in both seizure generation and the involvement of other brain regions such as the cortex.

In *Kcnq3* homozygous knockin mice bred to the FVBN genetic background, seizures continue into adulthood although they become less severe with age. This allowed us to uncover the important finding that early seizure-induced synaptic remodelling, such as mossy fibre sprouting, is not necessary for the persistence of the seizure phenotype. In fact, the *Kcnq3* neuropathology contrasts many current models of epileptogenesis in which synaptic reorganization of mossy fibres and loss of pyramidal and hilar neurons play a salient role in the generation of recurrent seizures (Ben-Ari & Holmes, 2006). Like these drug-induced epilepsy models, *Kcnq3* homozygous knockin mice exhibit putative neuroprotective responses such as enhanced expression of the inhibitory neuropeptide NPY (Scharfman & Gray, 2006).

Kcnq3$^{G311V/G311V}$ mice provide a very different seizure model when compared to *Kcnq2*$^{A306T/A306T}$ mice, despite the fact that the seizure characteristics are quite similar among patients that express either mutation (Ryan *et al.* 1991; Ronen *et al.* 1993; Singh *et al.* 2003). *Kcnq3*$^{G311V/G311V}$ mice experience frequent daily spontaneous seizures throughout development and into adulthood on the FVB inbred background

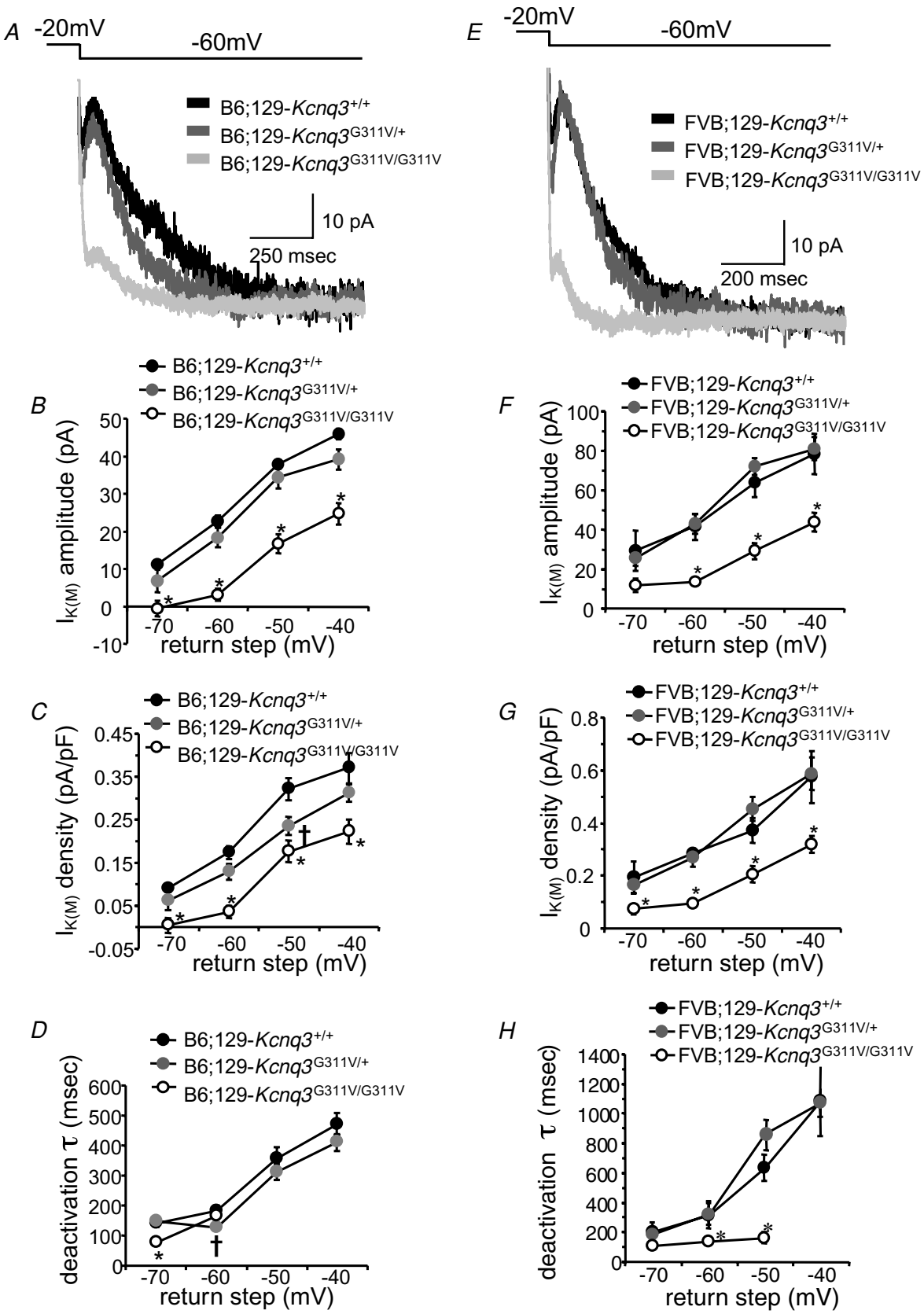

Figure 9. $I_{K(M)}$ amplitude and density are decreased in CA1 neurons of N1 B6;129-*Kcnq3*$^{G311V/G311V}$ and N1 FVB;129-*Kcnq3*$^{G311V/G311V}$ mice

but have rare seizures on the B6 inbred background. *Kcnq2*$^{A306T/A306T}$ mice bred to the FVB inbred strain exhibit early onset seizures that are lethal before postnatal day 20 and when bred to the B6 background, exhibit far fewer seizures during the monitored period. Moreover, *Kcnq3*$^{G311V/+}$ mice on the FVB background require less electrical stimulation to induce a tonic hindlimb extension seizure when compared to the B6 inbred genetic background. Such a profound difference in seizure susceptibility between the FVB and B6 mouse strains is supported by other measures of hyperexcitability and neurotoxicity as well as identified quantitative trait loci that most probably account for such variation (Ferraro *et al.* 2001; Frankel *et al.* 2001; Mori *et al.* 2004; Schauwecker *et al.* 2004). On the FVB background, seizures in *Kcnq3*$^{G311V/G311V}$ mice have a delayed onset, characterized by clonic activity that may or may not advance to tonic hindlimb extension, whereas seizures in *Kcnq2*$^{A306T/A306T}$ mice manifest almost instantaneous tonic hindlimb extension from the onset. The apparently more severe spontaneous seizures exhibited by *Kcnq2*$^{A306T/A306T}$ knockin mice characterized by a shorter seizure latency and increased seizure-related lethality may be due to the unique contributions of KCNQ2 to M-channel-mediated cellular and network synaptic properties. Since a significant proportion of the M-current is carried by homomeric KCNQ2 channels earlier in development, its unique capacity to limit intrinsic bursting may preferentially confer an increased seizure-related lethality in early postnatal mutant *Kcnq2* mice (Tinel *et al.* 1998; Hadley *et al.* 2003). Alternatively, the late postnatal expression of mutant KCNQ3 appears when inhibitory neurotransmitter systems such as GABA have already matured, which may reduce the severity of mutant KCNQ3-mediated seizures (Dzhala *et al.* 2005; Geiger *et al.* 2006). Finally, compared to KCNQ3, KCNQ2 expression is quantitatively higher and appears to have a broader spatial expression pattern in cellular compartments that are critical in controlling responses to synaptic input (Tinel *et al.* 1998; Devaux *et al.* 2004; Geiger *et al.* 2006; Pan *et al.* 2006; Weber *et al.* 2006). While both proteins are expressed in the hippocampus, cortex and thalamic reticular nucleus, the extrapyramidal and midbrain expression pattern is unique to KCNQ2-containing M-channels. This expression pattern coupled with the extensive nodal role of KCNQ2 could translate to a more rapid synchronization of bursting neurons leading to more severe tonic hindlimb extension seizures seen in *Kcnq2* mutant mice.

The present work demonstrates that the heterozygous mice with an S6 transmembrane domain mutation in *Kcnq2* or a pore mutation in *Kcnq3* exhibit enhanced seizure susceptibility concomitant with some changes in deactivation of the $I_{K(M)}$ current. In addition, homozygous mice display recurrent spontaneous seizures into adulthood with substantial changes in $I_{K(M)}$ amplitude, current density and deactivation kinetics, but in the absence of notable hippocampal pathology. Our findings emphasize the vital role that the KCNQ2- and KCNQ3-forming M-channel plays in controlling neuronal excitability and confirm our initial genetic observation that KCNQ2 and KCNQ3 malfunction can lead to seizures in patients. The results presented here confirm that both knockin mice are a valuable model system to study the unique disorder of BFNC and M-current hypofunctionality. In particular, the *Kcnq3* homozygous knockin mice on the FVB genetic background provide an unambiguous, reproducible seizure phenotype that can readily be used for the evaluation of mechanistically novel anti-epileptic drugs.

A, sample traces recorded from wild-type B6;129-*Kcnq3*$^{+/+}$ (black), heterozygous mutant B6;129-*Kcnq3*$^{G311V/+}$ (darker grey), and homozygous mutant B6;129-*Kcnq3*$^{G311V/G311V}$ (lighter grey) CA1 neurons in response to the −20 to −60 mV step. $I_{K(M)}$ amplitude is measured from the deactivation hump (10–20 ms after the hyperpolarizing step) to the steady-state level at the end of the trace. *B*, $I_{K(M)}$ amplitude is decreased relative to wild-type in B6;129-*Kcnq3*$^{G311V/G311V}$ CA1 neurons (*$P < 0.005$; all return steps). *C*, $I_{K(M)}$ density is also decreased in B6;129-*Kcnq3*$^{G311V/G311V}$ CA1 neurons (*$P < 0.005$; all return steps). At the −50 mV return step, $I_{K(M)}$ density is decreased in B6;129-*Kcnq3*$^{G311V/+}$ CA1 neurons relative to wild-type (†$P < 0.05$). *D*, $I_{K(M)}$ deactivation kinetics are faster in B6;129-*Kcnq3*$^{G311V/+}$ CA1 neurons than wild-type only at the −60 mV return step (†$P < 0.01$); in B6;129-*Kcnq3*$^{G311V/G311V}$ CA1 neurons, $I_{K(M)}$ deactivation is faster than wild-type only at the −70 mV step (*$P < 0.01$). *E*, sample traces recorded from wild-type FVB;129-*Kcnq3*$^{+/+}$ (black), heterozygous mutant FVB;129-*Kcnq3*$^{G311V/+}$ (darker grey), and homozygous mutant FVB;129-*Kcnq3*$^{G311V/G311V}$ (lighter grey) CA1 neurons in response to the −20 to −60 mV step. $I_{K(M)}$ amplitude is measured from the deactivation hump (10–20 ms after the hyperpolarizing step) to the steady-state level at the end of the trace. *F*, at the −60, −50 and −40 mV return steps, $I_{K(M)}$ amplitude is decreased relative to wild-type in FVB;129-*Kcnq3*$^{G311V/G311V}$ CA1 neurons (*$P < 0.005$). *G*, $I_{K(M)}$ density is decreased in FVB;129-*Kcnq3*$^{G311V/G311V}$ CA1 neurons at all return steps (*$P < 0.05$ for −70 mV step; $P < 0.01$ for −60, −50, −40 mV steps). *H*, $I_{K(M)}$ deactivation kinetics are faster in FVB;129-*Kcnq3*$^{G311V/G311V}$ CA1 neurons than wild-type at the −60 and −50 mV return step (*$P < 0.05$); in FVB;129-*Kcnq3*$^{G311V/+}$ CA1 neurons, $I_{K(M)}$ deactivation is similar to wild-type.

References

Ben-Ari Y & Holmes GL (2006). Effects of seizures on developmental processes in the immature brain. *Lancet Neurol* **5**, 1055–1063.

Biervert C, Schroeder BC, Kubisch C, Berkovic SF, Propping P, Jentsch TJ & Steinlein OK (1998). A potassium channel mutation in neonatal human epilepsy. *Science* **279**, 403–406.

Blume WT (2006). The progression of epilepsy. *Epilepsia* **47**, 71–78.

Bunting M, Bernstein KE, Greer JM, Capecchi MR & Thomas KR (1999). Targeting genes for self-excision in the germ line. *Genes Dev* **13**, 1524–1528.

Charlier C, Singh NA, Ryan SG, Lewis TB, Reus BE, Leach RJ & Leppert M (1998). A pore mutation in a novel KQT-like potassium channel gene in an idiopathic epilepsy family [see comments]. *Nat Genet* **18**, 53–55.

Chung HJ, Jan YN & Jan LY (2006). Polarized axonal surface expression of neuronal KCNQ channels is mediated by multiple signals in the KCNQ2 and KCNQ3 C-terminal domains. *Proc Natl Acad Sci U S A* **103**, 8870–8875.

Devaux JJ, Kleopa KA, Cooper EC & Scherer SS (2004). KCNQ2 is a nodal K^+ channel. *J Neurosci* **24**, 1236–1244.

Dzhala VI, Talos DM, Sdrulla DA, Brumback AC, Mathews GC, Benke TA, Delpire E, Jensen FE & Staley KJ (2005). NKCC1 transporter facilitates seizures in the developing brain. *Nat Med* **11**, 1205–1213.

Ferraro TN, Golden GT, Smith GG, Longman RL, Snyder RL, DeMuth D, Szpilzak I, Mulholland N, Eng E, Lohoff FW, Buono RJ & Berrettini WH (2001). Quantitative genetic study of maximal electroshock seizure threshold in mice: evidence for a major seizure susceptibility locus on distal chromosome 1. *Genomics* **75**, 35–42.

Frankel WN, Taylor L, Beyer B, Tempel BL & White HS (2001). Electroconvulsive thresholds of inbred mouse strains. *Genomics* **74**, 306–312.

Geiger J, Weber YG, Landwehrmeyer B, Sommer C & Lerche H (2006). Immunohistochemical analysis of KCNQ3 potassium channels in mouse brain. *Neurosci Lett* **400**, 101–104.

Hadley JK, Passmore GM, Tatulian L, Al-Qatari M, Ye F, Wickenden AD & Brown DA (2003). Stoichiometry of expressed KCNQ2/KCNQ3 potassium channels and subunit composition of native ganglionic M channels deduced from block by tetraethylammonium. *J Neurosci* **23**, 5012–5019.

Lucarini N, Verrotti A, Napolioni V, Bosco G & Curatolo P (2007). Genetic polymorphisms and idiopathic generalized epilepsies. *Pediatric Neurol* **37**, 157–164.

Michalakis M, Holsinger D, Ikeda-Douglas C, Cammisuli S, Ferbinteanu J, DeSouza C, DeSouza S, Fecteau J, Racine RJ & Milgram NW (1998). Development of spontaneous seizures over extended electrical kindling. I. Electrographic, behavioral, and transfer kindling correlates. *Brain Res* **793**, 197–211.

Mori M, Burgess DL, Gefrides LA, Foreman PJ, Opferman JT, Korsmeyer SJ, Cavalheiro EA, Naffah-Mazzacoratti MG & Noebels JL (2004). Expression of apoptosis inhibitor protein Mcl1 linked to neuroprotection in CNS neurons. *Cell Death Differ* **11**, 1223–1233.

Nagy A, Rossant J, Nagy R, Abramow-Newerly W & Roder JC (1993). Derivation of completely cell culture-derived mice from early-passage embryonic stem cells. *Proc Natl Acad Sci U S A* **90**, 8424–8428.

Otto JF, Yang Y, Frankel WN, White HS & Wilcox KS (2006). A spontaneous mutation involving Kcnq2 (Kv7.2) reduces M-current density and spike frequency adaptation in mouse CA1 neurons. *J Neurosci* **26**, 2053–2059.

Otto JF, Yang Y, Frankel WN, Wilcox KS & White HS (2004). Mice carrying the szt1 mutation exhibit increased seizure susceptibility and altered sensitivity to compounds acting at the m-channel. *Epilepsia* **45**, 1009–1016.

Pan Z, Kao T, Horvath Z, Lemos J, Sul JY, Cranstoun SD, Bennett V, Scherer SS & Cooper EC (2006). A common ankyrin-G-based mechanism retains KCNQ and NaV channels at electrically active domains of the axon. *J Neurosci* **26**, 2599–2613.

Peters HC, Hu H, Pongs O, Storm JF & Isbrandt D (2005). Conditional transgenic suppression of M channels in mouse brain reveals functions in neuronal excitability, resonance and behavior. *Nat Neurosci* **8**, 51–60.

Rett A & Teubel R (1964). Neugeborenenkrämpfe im Rahmen einer epileptisch belasteten Familie. *Wien Klin Wochenschr* **76**, 609–613.

Ronen GM, Rosales TO, Connolly M, Anderson VE & Leppert M (1993). Seizure characteristics in chromosome 20 benign familial neonatal convulsions. *Neurology* **43**, 1355–1360.

Ryan SG, Wiznitzer M, Hollman C, Torres MC, Szekeresova M & Schneider S (1991). Benign familial neonatal convulsions: evidence for clinical and genetic heterogeneity. *Ann Neurol* **29**, 469–473.

Scharfman HE & Gray WP (2006). Plasticity of neuropeptide Y in the dentate gyrus after seizures, and its relevance to seizure-induced neurogenesis. *EXS* **95**, 193–211.

Schauwecker PE, Williams RW & Santos JB (2004). Genetic control of sensitivity to hippocampal cell death induced by kainic acid: a quantitative trait loci analysis. *J Comp Neurol* **477**, 96–107.

Schroeder BC, Kubisch C, Stein V & Jentsch TJ (1998). Moderate loss of function of cyclic-AMP-modulated KCNQ2/KCNQ3 K^+ channels causes epilepsy. *Nature* **396**, 687–690.

Shah MM, Mistry M, Marsh SJ, Brown DA & Delmas P (2002). Molecular correlates of the M-current in cultured rat hippocampal neurons. *J Physiol* **544**, 29–37.

Singh NA, Charlier C, Stauffer D, DuPont BR, Leach RJ, Melis R *et al.* (1998). A novel potassium channel gene, KCNQ2, is mutated in an inherited epilepsy of newborns [see comments]. *Nat Genet* **18**, 25–29.

Singh NA, Westenskow P, Charlier C, Pappas C, Leslie J, Dillon J, Anderson VE, Sanguinetti MC & Leppert MF (2003). KCNQ2 and KCNQ3 potassium channel genes in benign familial neonatal convulsions: expansion of the functional and mutation spectrum. *Brain* **126**, 2726–2737.

Thomas KR & Capecchi MR (1987). Site-directed mutagenesis by gene targeting in mouse embryo-derived stem cells. *Cell* **51**, 503–512.

Tinel N, Lauritzen I, Chouabe C, Lazdunski M & Borsotto M (1998). The KCNQ2 potassium channel: splice variants, functional and developmental expression. Brain localization and comparison with KCNQ3. *FEBS Lett* **438**, 171–176.

Wang HS, Pan Z, Shi W, Brown BS, Wymore RS, Cohen IS, Dixon JE & McKinnon D (1998). KCNQ2 and KCNQ3 potassium channel subunits: molecular correlates of the M-channel [see comments]. *Science* **282**, 1890–1893.

Watanabe H, Nagata E, Kosakai A, Nakamura M, Yokoyama M, Tanaka K & Sasai H (2000). Disruption of the epilepsy KCNQ2 gene results in neural hyperexcitability. *J Neurochem* **75**, 28–33.

Weber YG, Geiger J, Kampchen K, Landwehrmeyer B, Sommer C & Lerche H (2006). Immunohistochemical analysis of KCNQ2 potassium channels in adult and developing mouse brain. *Brain Res* **1077**, 1–6.

White HS (2002). Animal models of epileptogenesis. *Neurology* **59**, S7–S14.

Woodbury LA & Swinyard CA (1952). Stimulus parameters for electroshock seizures in rats. *Am J Physiol* **170**, 661–667.

Yang Y, Beyer BJ, Otto JF, O'Brien TP, Letts VA, White HS & Frankel WN (2003). Spontaneous deletion of epilepsy gene orthologs in a mutant mouse with a low electroconvulsive threshold. *Human Mol Genet* **12**, 975–984.

Yue C & Yaari Y (2004). KCNQ/M channels control spike afterdepolarization and burst generation in hippocampal neurons. *J Neurosci* **24**, 4614–4624.

Acknowledgements

This work was supported in part by grants from the NIH (RO1 NS-32666 to M.F.L, RO1 NS-44210 to K.S.W. and RO1 NS-29709/MMDDRC HD-24064 to J.L.N.), the W. Keck Foundation (to M.F.L), and the Primary Children's Medical Center Foundation (K.S.W.). We wish to thank the ARUP Laboratories, Sheryl Tripp, Blake Anderson, Kirk Thomas, Joy Greer, Michaeline Bunting, Brith Otterud, Tiffany Buge and France Davis for their valuable contributions to the project. Images were obtained at the University of Utah School of Medicine Cell Imaging Facility. Knockin mice were made in conjunction with the University of Utah Transgenic Core Facility.

Supplemental material

Online supplemental material for this paper can be accessed at:
http://jp.physoc.org/cgi/content/full/jphysiol.2008.154971/DC1
and
http://www.blackwell-synergy.com/doi/suppl/10.1113/jphysiol.2008.154971